Variable-speed Single-phase Induction Motor Drive for Vehicular Applications

Valery Vodovozov, Nikolai Lillo, Zoja Raud

Tallinn University of Technology
Ehitajate tee, 5, 19086, Tallinn, Estonia
valery.vodovozov@ttu.ee

Received 30 November, 2013; Revised 2 January, 2014; Accepted 5 February, 2014; Published 20 April, 2014

Abstract

Despite of popularity and multiple attractive features, a single-phase induction motor (SPIM) still not used in the vehicular applications because of starting problems, low-speed operation complexity, and other control drawbacks. The aim of this work is to realize the stable torque-speed characteristics of the low-power capacitor-run SPIM in wide range of speeds. The SPIM behavior at the variable-frequency operation was explored in the paper and some methods were proposed to improve the motor characteristics. To overcome the prominent shortcomings and to meet the vehicle requirements, some novelties were designed in the SPIM control arrangements.

Keywords

Vehicle Applications; Electric Drive; Single-phase Induction Motor; Propulsion Drive; Auxiliary Vehicle Systems

Introduction

Nowadays, much research has been done in the field of the future vehicle technologies. The automotive industry has turned to the market of electric drives. This has motivated researchers to focus on design and development of new architectures for vehicle electric systems. The alternating and direct current motor drives over a wide range of powers and speeds fed by power converters have become an inherent part of the vehicle embedded systems (Fahimi, 2007; Vodovozov, 2013). Electric drives became relevant not only for cars, but also for many task-oriented two- and three-wheelers.

As follows from the contemporary vehicle specifications, the general tendency in their design is toward higher efficiency, weight reduction, and additional functionalities (Shaout, 2013; Vodovozov, 2012). Therefore during the last decade many hydraulics systems have been removed and replaced with electric ones. The 42 V on-board supplies of the new car brands opened the extended possibilities in efficiency and comfort growth along with loss, current, size, weight, and noise reduction of the auxiliary vehicle systems.

Various approaches for the low-power vehicle drives classification may be proposed.

On the one hand, all such drives can be divided as the propulsion and the auxiliary devices. The small propulsion systems are used mainly in two-wheelers, primarily bikes and scooters, whereas the list of the auxiliary low-power drives is very diverse. Currently, a car can count from 30 to 170 auxiliary electric machines occupying the very wide power range, from watts to few kilowatts (Ombach, 2010). Along with the traditional driving equipment, such as electric steering systems, engine coolers, dual-clutch actuators, windshield wipers, window lifters, seat and mirror adjustment devices, fans, pumps for oil, fuel, and water supply, electrical brakes, suspension systems, gate openers, etc., the new devices appear, for example electric air-conditioning compressors, airgates, x-by-wire systems, air blowers, fluid pumps for the fuel cell supplied vehicles, etc (Goodarzi, 2005).

On the other hand, the low-power drives may be ranged between the systems with the small start-up torque and the systems with the considerable start-up requirements. The former group envelops multiple auxiliary pumps, fans, and compressors as well as some propulsion systems of bicycles operated under the rider pedalling. The remaining equipment relates to the latter group.

This large spectrum of embedded electric drives is

covered with different technologies, where both the outdated brushed and the modest brushless induction and synchronous motors are used. The brushed machines are no longer the preferable option for vehicle applications because of their low efficiency and power-to-weight ratio, high maintenance, and high-speed performance limitation. On the contrary, the permanent magnet brushless motors were considered as the suitable machines thanks to their efficiency for most vehicle auxiliary applications from Toyota, Honda, and some other firms, including the bike manufacturers. Nevertheless, the positioning sensor and three-phase design significantly increase the overall cost and size of a vehicle and decrease its reliability. The permanent magnets and position sensors are sensitive to high temperatures, humidity, and vibrations (Knezevic, 2013). Some of these drawbacks are overcoming with the switched reluctance motors although they bring some another problems.

At the same time, multiple three-phase induction motors are well accepted by Ford, General Motors, other companies, and two-wheeler vendors thanks to their wide speed range, simple design, ruggedness, and less cost.

In terms of cost, size, and weight reduction as well as increase in reliability, the single-phase induction motors (SPIM) attract much attention in different areas, excepting the vehicular applications. Among the SPIM types, the shaded-pole, split-phase, permanent split-capacitor (also known as single-value capacitor), and two-value capacitor motors are popular. The main differences in their design consider the methods of the running torque producing.

Since it is no rotating magnetic field in the SPIM, it cannot start without modification. The most common type of aid used to run a SPIM is the starting capacitor installed in series with the auxiliary winding to realize another phase from the supply source and to feed an auxiliary winding so that the motor could operate as a balanced two-phase machine. For this purpose the capacitor size must be carefully determined according to the terminal impedance of the auxiliary winding. Essentially, the capacitor-run SPIM is a single-speed device normally operated at the fixed-frequency supply because its impedance depends on the supply frequency and is changing along with a speed. This confirms that the proper capacitor value is important not only for running but for the steady-state operation because it defines optimal performance at different frequencies.

The open-loop voltage-frequency control applied for the three-phase induction motor drives is difficult to use for speed adjustment of the capacitor-run SPIM because at low frequencies the capacitor reactance grows exponentially and current seeks to zero. To keep the auxiliary winding current at the nominal level, it is required to raise the supply voltage or to decrease the impedance. By-turn, at the common supply of both the main and the auxiliary windings, an increase of voltage will raise the current in the main winding over its nominal value.

On the contrary, with the capacitance adjustment, the current could be balanced and stable in both the main and the auxiliary windings. Several methods of capacitance regulation in SPIM applications are known (Lettenmainer, 1988; Liu, 1993; Sunter, 2011). For a long time, divers techniques for the starting torque increasing and the smooth acceleration capability management are discussed.

The current work aims to justify an approach to design the torque-speed characteristics of SPIM required for various vehicle drive systems at a broad speed range. The goal of the paper is to demonstrate some methods of the capacitor-run SPIM adjustment providing the stable torque and speed regulation at different frequencies within the open-loop drive topology.

Study the SPIM with Permanent Capacitor in Auxiliary Winding

To analyse the capacitor-run SPIM behavior, a mathematical model has been developed in the Matlab/Simulink software environment. The replacement circuits of the two-winding SPIM are shown in Fig. 1 (MathWorks, 2012): the main winding (a) and the auxiliary one (b).

The dynamic mathematical model of the same machine can be described using the following set of equations (Krause, 2013):

$$V_{qs} = R_s i_{qs} + \frac{d\varphi_{qs}}{dt} \quad (1)$$

$$V_{ds} = R_S i_{ds} + \frac{d\varphi_{ds}}{dt} \quad (2)$$

$$0 = R'_r i'_{qr} + \frac{d\varphi'_{qr}}{dt} - \left(\frac{N_s}{N_S}\right)\omega_r \varphi'_{dr} \quad (3)$$

$$0 = R'_R i'_{dr} + \frac{d\varphi'_{dr}}{dt} - \left(\frac{N_S}{N_s}\right)\omega_r \varphi'_{qr} \quad (4)$$

$$T_e = p\left[\left(\frac{N_S}{N_s}\right)\varphi'_{qr} i'_{dr} - \left(\frac{N_s}{N_S}\right)\varphi'_{dr} i'_{qr}\right] \quad (5)$$

where

$$\varphi_{qs} = L_{ss} i_{qs} + L_{ms} i'_{qr} \quad (6)$$

$$\varphi_{ds} = L_{SS} i_{ds} + L_{mS} i'_{dr} \quad (7)$$

$$\varphi'_{qr} = L'_r i'_{qr} + L_{ms} i_{qs} \quad (8)$$

$$\varphi'_{dr} = L'_{RR} i'_{dr} + L_{mS} i_{ds} \quad (9)$$

$$L_{ss} = L_{ls} + L_{ms} \quad (10)$$

$$L_{SS} = L_{lS} + L_{mS} \quad (11)$$

$$L'_{rr} = L'_{lr} + L_{ms} \quad (12)$$

$$L'_{RR} = L'_{lR} + L_{mS} \quad (13)$$

Here, *Rs* and *Lls* are the stator resistance and leakage inductance of the main winding; *RS* and *LlS* are the stator resistance and leakage inductance of the auxiliary winding; *R'r* and *L'lr* are the rotor resistance and leakage inductance of the main winding; *R'R* and *L'lR* are the rotor resistance and leakage inductance of the auxiliary winding; *Lms* and *LmS* are the magnetizing inductances of the main and auxiliary windings; *Lss* and *L'rr* are the total stator and rotor inductances of the main winding; *LSS* and *L'RR* are the total stator and rotor inductances of the auxiliary winding; *Vqs* and *iqs* are the q-axis stator voltage and current; *Vds* and *ids* are the *d*-axis stator voltage and current; *V'dr* and *I'dr* are the *d*-axis rotor voltage and current; *V'qr* and *I'qr* are the *q*-axis rotor voltage and current, ϕqs and ϕds are the stator *q*- and *d*-axes fluxes, $\phi' qr$ and $\phi' dr$ are the rotor *q*- and *d*-axes fluxes, *p* is the number of pole pairs, *Te* is the electromagnetic torque, *Ns*, *NS* are the number of main and auxiliary winding effective turns.

The motor data used for simulation are listed in Table1. An appropriate Simulink model is shown in Fig. 2. Here, the parallel-connected main (M+, M-) and auxiliary (A+, A-) motor windings are supplied from the universal PWM bridge inverter. The permanent 4μF capacitor (C) is added to the auxiliary winding circuit.

The motor electromagnetic torque *Te* and the rotor angular speed ωr were observed in simulation. The simulated torque-speed curves at different frequencies are presented in Fig. 3. Simulation shows that at low frequencies the torque almost equals zero and the torque-speed characteristic of the motor is very smooth. As a result, the motor cannot run and does not have enough torque to keep the constant load.

An effect of electromagnetic torque lowering along with the frequency drop can be explained using the torque equilibrium (5). The torque of the capacitor-run induction motor depends on the currents in both the main and the auxiliary windings. Along with the frequency decrease, an impedance of the auxiliary winding grows because of the series-connected capacitor, which reactance

$$X_C = \frac{1}{2\pi fC} \quad (14)$$

is inversely proportional to the frequency. At the same time, an impedance of the main winding decreases at low frequencies, that is

$$X_L = 2\pi fL. \quad (15)$$

Using the above model, the torque, speed, and current waveforms were observed at 10 Hz with the permanent 4 μF capacitor. The appropriate diagrams are presented in Fig. 4.

This simulation has confirmed that at low frequencies the small capacitor reactance affects negatively the auxiliary winding current, which reaches zero. As a result, the motor does not produce the torque and, after applying the nominal load for about 0.5 s the motor cannot run or begins to rotate in the reverse direction.

According to the simulation results, the SPIM with a permanent capacitor can be recommended for the vehicle systems with the small start-up torque, primarily for the auxiliary pumps, fans, and compressors as well as for the propulsion systems of bicycles operated under the rider pedalling.

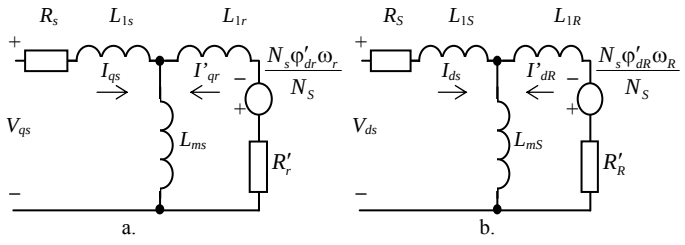

FIG. 1 REPLACEMENT CIRCUITS OF SPIM

TABLE 1 MOTOR RATINGS AND PARAMETERS

Rating, parameter	Value
P_n	50 W
U_n	220 V
I_n	0.37 A
f_n	50 Hz
n_n	2780 rpm
R_s	85 Ω
R_S	60 Ω
L_s	580 mH

Rating, parameter	Value
L_S	460 mH
N_s/N_S	1.18
L_{ms}	1.1 H
J_n	0.00005 kgm^2
p	1
C	4 μF

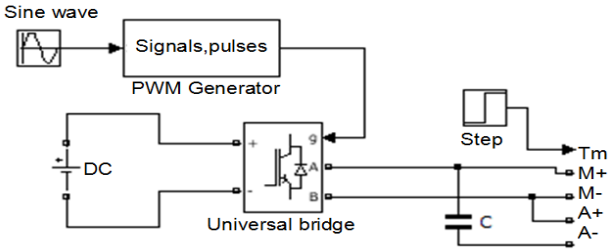

FIG. 2 SIMULINK MODEL WITH PERMANENT CAPACITOR

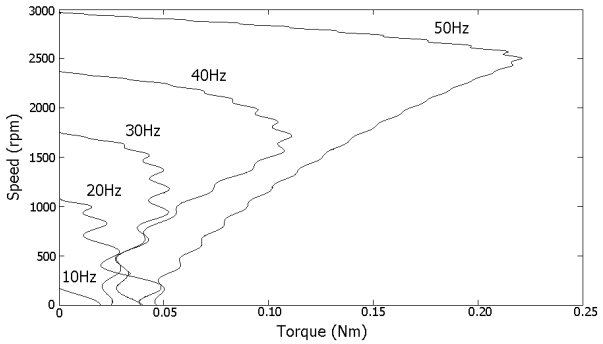

FIG. 3 SIMULATED TORQUE-SPEED CURVES WITH CONSTANT CAPACITOR OF 4μF IN THE FREQUENCY RANGE OF 10 – 50 HZ

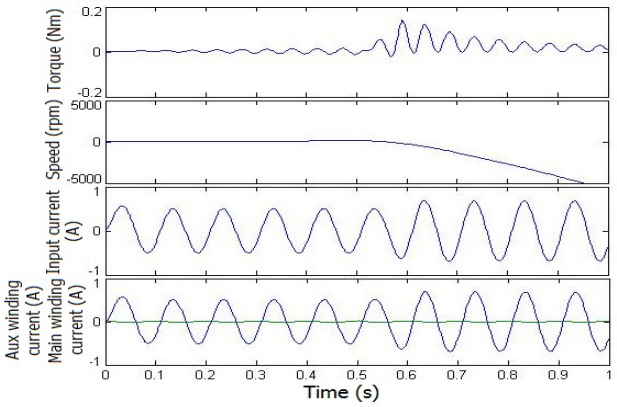

FIG. 4 SIMULATED TORQUE, SPEED, AND CURRENT WAVEFORMS WITH PERMANENT 4 μF CAPACITOR AT 10 HZ

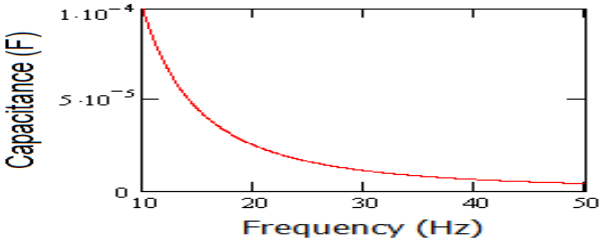

FIG. 5 OPTIMAL VALUE OF CAPACITANCE FOR MAXIMAL TORQUE IN THE FREQUENCY RANGE OF 10 – 50 HZ

STUDY the SPIM with Variable Capacitance

To resolve the problem and support the constant $\frac{X_C}{X_L}$ ratio, the capacitance should be changed along with the change of the main winding reactance as shown in Fig. 5. With exponential change, it reaches approximately 100μF at 10 Hz.

In many vehicle systems with normal start-up requirements, the motor should operate within an average speed range at the nominal torque with the minimal losses and maximal efficiency. To meet these requirements, it is reasonable to use a schematic with two parallel-connected adjusted capacitors in the auxiliary winging. The best way to change the capacitance is to introduce the PWM-controlled choppers into the capacitor arms. Using these choppers, the capacitors can be switched on and off respectively thus supporting minimal switching losses.

A scheme of such a circuit is presented in Fig. 6. A couple of capacitors, C1 of low capacitance and C2 of high capacitance, are used in the system. Each of them is connected in series with an auxiliary winding through the choppers S5 and S6 controlled by PWM with a frequency of about 1 kHz. The capacitance is changed by variation of the duty cycle $x = \frac{t_{on}}{t_{on} + t_{off}}$ from 0 to 1. The switch S6 is connected with an inverted logic with respect to S5, which means that only one switch is in the on state at the moment. By lowering the duty cycle, more current can be directed to the capacitor C2 and less to C1. In this way, the current in the auxiliary winding is changed along with the duty cycle adjustment.

Energy stored in the capacitors can be expressed as

$$E = \frac{CU^2}{2}. \quad (16)$$

From (16), the capacitance needed at the particular duty cycle can be calculated as follows:

$$C_{needed} = C_1 \cdot x^2 + C_2 \cdot (1-x)^2. \quad (17)$$

Fig. 7 illustrates the dependence of capacitance on the duty cycle.

This non-linear curve has the similar shape as in Fig. 5. Their comparison shows that the duty cycle of the choppers in the capacitor circuits should be proportionally changed along with the frequency adjustment.

The choppers and the capacitors with the appropriate

gate driver were introduced to the Simulink model. The results of the system simulation are shown in Fig. 8. Now, the torque-speed curves became more stable within the above discussed frequency range.

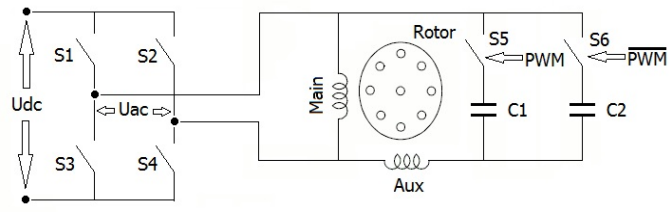

FIG. 6 CIRCUIT WITH INVERTER, MOTOR, AND SWITCHED CAPACITOR

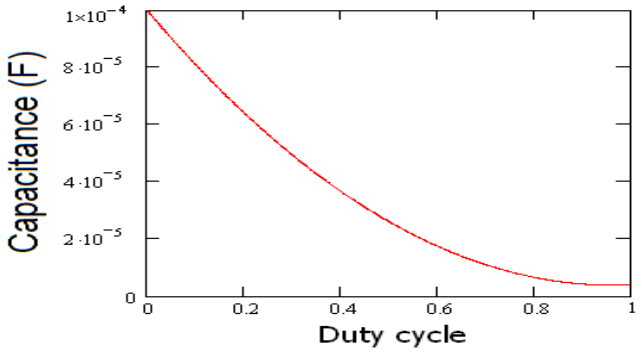

FIG. 7 REQUIRED CAPACITANCE VS. DUTY CYCLE

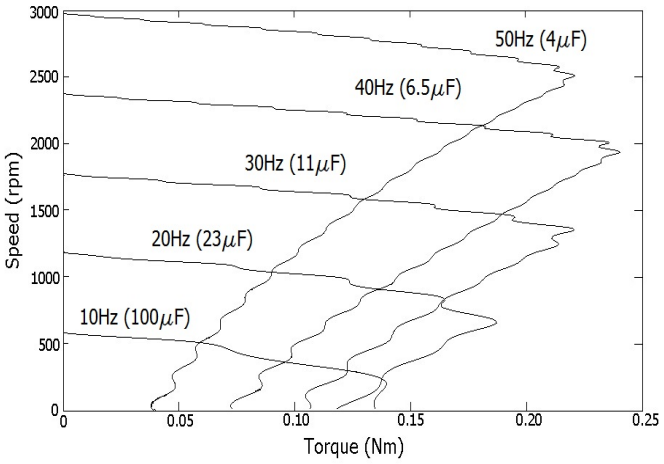

FIG. 8 SIMULATED TORQUE-SPEED CURVES WITH VARIABLE CAPACITANCE IN THE FREQUENCY RANGE OF 10 – 50 HZ

Boosting and Slip Compensation

Nevertheless, the motor still cannot keep the nominal torque at the frequencies below 10 Hz. The reason is again in the stator winding impedance, which has an active resistance. During the voltage-frequency control, the voltage changes linearly and at the lower frequencies the current does not reach its nominal value. To resolve the problem, it was proposed to keep the current constant at low frequencies by boosting the supply voltage. In the model the boosting level was varied from 5% at 20 Hz to 25% at 10 Hz.

With boosting, the torque-speed curves have became stable in the full frequency range and torque is stable even at low frequencies (Fig. 9).

Fig. 10 presents the simulated torque, speed, and currents waveforms at 10 Hz with switched capacitance and boosting. The traces show that the motor keeps the proper rotation direction even after applying the nominal load and the currents do not exceed their permitted values in both the main and the auxiliary windings.

Nevertheless, such responsible auxiliary vehicle drives as electric power steering systems and electrical brakes need in the broader speed range. To get the harder torque-speed characteristics of the drive system, it is important to control not only the torque. It is therefore required to reduce the slip of induction motor to maintain its stable work even at very low frequencies and high loads. The slip is defined as follows:

$$s = \frac{n_s - n_r}{n_s} \tag{18}$$

where ns is the synchronous speed and nr is the rotor mechanical speed.

As shown in Fig. 8, the relation between torque and slip is almost linear until the nominal torque. Using the motor passport data, the drive nominal slip can be counted as 7.3 % in the above example. As soon as the passport torque is known, the slip compensation coefficient can be established in this case as 2.5 Hz/Nm.

Now, at any load variation this coefficient can be taken into account to correct the reference speed. To test this proposition, simulation has been done. The initial speed response of the system on the torque applying at 0.5 s without the slip compensation is shown in Fig. 11, a. With the slip compensation at the motor loading with half of the nominal load, the results are shown in Fig 11, b and with the nominal load – in Fig. 11, c. The simulation shows that the stable speed was obtained at different loads.

Experimental Results

For experimental testing, the capacitor-run SPIM KD-50 motor was rigidly coupled with the three-phase loading induction machine fed from PowerFlex 40. For the measurements, an oscilloscope Hantek DSO5102p, current probes Fluke i80-110s, and a tachometer were used. First, the testing SPIM was connected with the 4 μF capacitor through the switching chopper S5. Two measurements at 10 Hz and at 50 Hz were realized. Fig. 12 confirms that at 10 Hz with a 4 μF capacitor the

current in the auxiliary winding almost equals zero. The motor cannot start below 20 Hz and runs only when the frequency increases.

After changing the capacitance to 100 μF and applying the 25 % boosting, the current in the auxiliary winding reaches its nominal value. The motor starts to rotate in the proper direction and keeps the nominal torque all the way. The results of the experimental study are collected in Table 2.

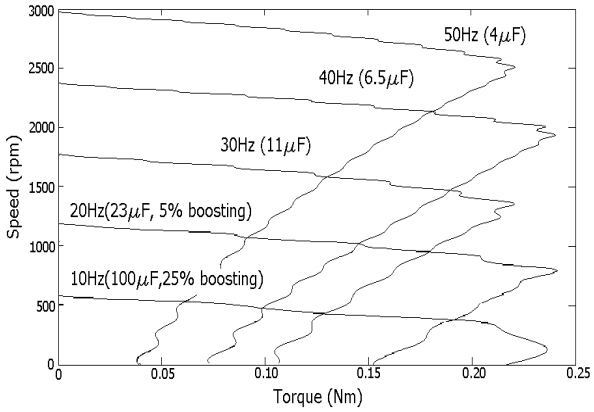

FIG. 9 SIMULATED TORQUE-SPEED CURVES WITH VARIABLE CAPACITANCE AND BOOSTING IN THE FREQUENCY RANGE OF 10 – 50 HZ.

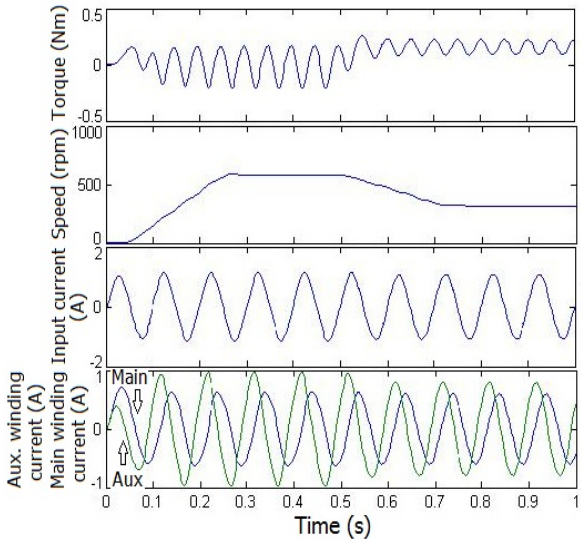

FIG. 10 SIMULATED TORQUE, SPEED AND CURRENTS WAVEFORMS WITH VARIABLE CAPACITANCE AND BOOSTING AT THE FREQUENCY OF 10 HZ.

TABLE 2 MOTOR SPEEDS

Condition	Speed, rpm
10 Hz, 4 μF, without load	0
10 Hz, 4 μF, rated load	Negative rotation
50 Hz, 4 μF, without load	2973
50 Hz, 4 μF, rated load	2768
10 Hz, 100 μF, without load	542
10 Hz, 100 μF, rated load	279

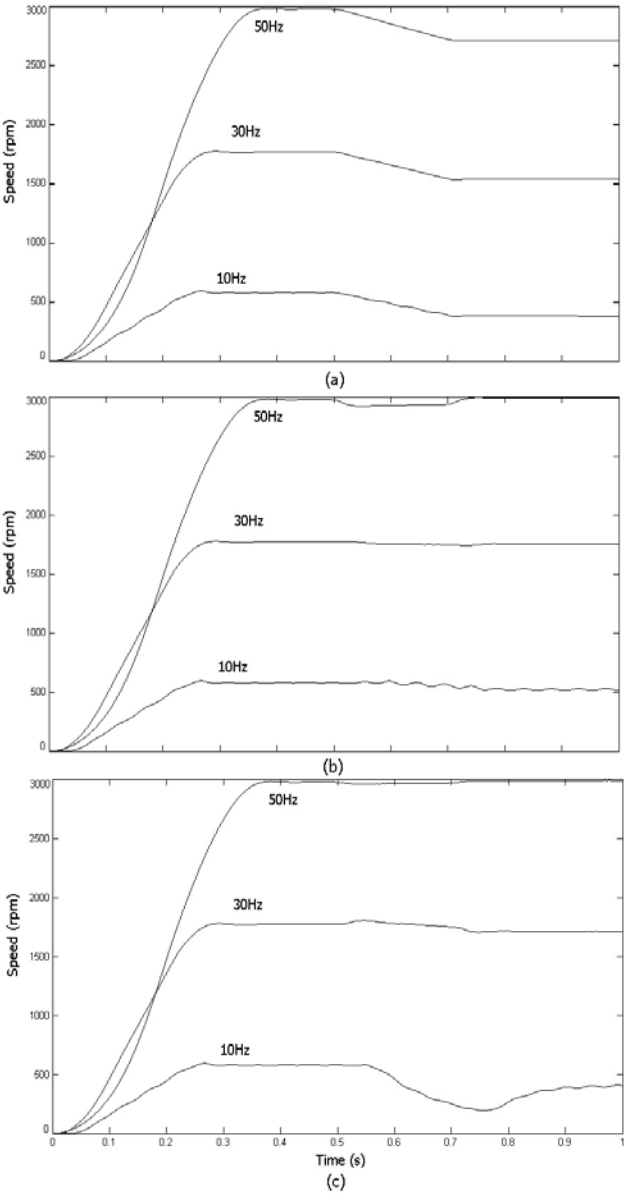

FIG. 11 SIMULATED SLIP COMPENSATION AT DIFFERENT FREQUENCIES: (A) – WITHOUT COMPENSATION, LOAD 0.16 NM, (B) – WITH COMPENSATION, LOAD 0.07 NM, (C) – WITH COMPENSATION, LOAD 0.16 NM.

Conclusions

The single-phase electric drives proposed in the paper can improve the performance characteristics of the vehicular applications. Some of them are suitable for the bike propulsion and for the vehicle pumps, fans, and compressors. Another low-power capacitor-run SPIMs, thanks to the obtained stable torque-speed characteristics can operate in the full range of speeds and loads that meet the vehicle embedded system requirements. Thanks to low cost, size, and weight, they have benefits as compared to the three-phase and brushless motors of the bikes and many auxiliary vehicle drives.

ACKNOWLEDGMENT

This research work has been supported by the Estonian Ministry of Education and Research (Project SF0140016s11).

REFERENCES

Goodarzi, G. A. and Rush, J. "Integrated auxiliary drives for fuel cell vehicles." IEEE Conference on Vehicle Power and Propulsion. Chicago, Il, 2005, pp. 619 – 623.

Fahimi, B. and Sebastian, T., "Guest editorial special section on automotive electromechanical converters." IEEE Transactions on Vehicular Technology. Vol. 56, no. 4, 2007, pp. 1470–1476.

Knezevic, J. M. "Low-cost low-resolution sensorless positioning of dc motor drives for vehicle auxiliary applications." IEEE Transactions on Vehicular Technology. Vol. 62, no. 9, 2013, pp. 4328 – 4335.

Krause, P. C., Wasynczuk, O., Sudhoff, S. D. and Pekarek, S. Analysis of Electric Machinery and Drive Systems. Wiley-IEEE Press, 2013, 680 p.

Lettenmainer, A., Novotny, D. and Lipo, T. A. "Single-phase induction motor with an electronically controlled capacitor." IEEE Transactions on Industry Applications. 1988, Vol. 27, no 1, pp. 38 – 43.

Liu, T. H., Zhao, Y., Lipo, T. A. and Muljadi, E. "Adjustable AC capacitor for a single-phase induction motor." IEEE Transactions on Industry Applications. Vol. 29, no. 3, 1993, pp. 479 – 485.

MathWorks. Single Phase Asynchronous Machine (2012). http://www.mathworks.se/help/physmod/sps/powersys/ref/singlephaseasynchronousmachine.html.

Ombach, G. and Junak, J. "Weight and efficiency optimization of auxiliary drives used in automobile." 19th International Conference on Electrical Machines ICEM 2010. Rome, Italy, 2010, pp. 1 – 6.

Sunter, S., Ozdemir, M. and Gumus, B. "Modelling and simulation of single phase induction motor with adjustable switched capacitor." 9th International Conference of Power Electronic and Motion APEIE 2011. Bodrum, Turkey, 2011, pp. 19 – 27.

Shaout, A. and McGirr, K. "Real-time systems in automotive applications: Vehicle stability control." Electrical Engineering Research. Vol. 1, no. 4, 2013, pp. 83 – 95.

Vodovozov, V., Raud, Z. and Lehtla, T. "A toolbox to design inverters for automotive applications." 11th World Conference on Applications of Electrical Engineering AEE 2012. Vouliagmeni, Athens, Greece, 2012, pp. 190 – 195.

Vodovozov, V. "Scientific platforms to explore and test the drives of electric cars." 13th International Symposium "Topical Problems in the Field of Electrical and Power Engineering." Doctoral School of Energy and Geotechnology II, Parnu, Estonia, 2013, pp. 42 – 47.

Valery Vodovozov is a full professor in the Electrical Engineering Department of Tallinn University of Technology. At present, he teaches courses in electric drives and power electronics. His current research is in applications of automotive electric drives, electronics, and intellectual information systems. Prof. Vodovozov has more than 35 years of experience in teaching and conducting research in the electrical engineering and information technology fields at Tallinn University of Technology and St. Petersburg Electrotechnical University. He has published above 250 papers in topics related to electrical engineering, computer programming, and engineering education. Valery Vodovozov has obtained engineering and PhD in Electrical Engineering from St. Petersburg Electrotechnical University, Russia, in 1972 and 1980, respectively.

Nikolai Lillo is a PhD student at Tallinn University of Technology in the Electrical Engineering Department. His research work is devoted to electronics and motor drives. His thesis topic is "Research and improvement of motor drives for electric vehicles with on-board battery".

Zoja Raud is an assistant of Tallinn University of Technology where she serves in the Electrical Engineering Department since 1983. She received education in St. Petersburg State University and Institute of Economic and Management and obtained the PhD degree in Electrical Engineering from Tallinn University of Technology. Her current research is devoted to the development of educational technologies in the field of electrical drives and power electronics. Zoja Raud has presented the papers in several international conferences and participated in a number of research projects in the field of power electronics.